Published in final edited form as:
Cell. 2010 December 10; 143(6): 951–965. doi:10.1016/j.cell.2010.11.017.

Dynamics of cullin-RING ubiquitin ligase network revealed by systematic quantitative proteomics

Eric J. Bennett[1], **John Rush**[2], **Steven P. Gygi**[3], and **J. Wade Harper**[1]

[1] Department of Pathology, Harvard Medical School, Boston MA 02115

[3] Department of Cell Biology, Harvard Medical School, Boston MA 02115

[2] Cell Signaling Technologies, Danvers, MA 01923

Abstract

Dynamic reorganization of signaling systems frequently accompany pathway perturbations, yet quantitative studies of network remodeling by pathway stimuli are lacking. Here, we report the development of a quantitative proteomics platform centered on multiplex Absolute Quantification (AQUA) technology to elucidate the architecture of the cullin-RING ubiquitin ligase (CRL) network and to evaluate current models of dynamic CRL remodeling. Current models suggest that CRL complexes are controlled by cycles of CRL deneddylation and CAND1 binding. Contrary to expectations, acute CRL inhibition with MLN4924, an inhibitor of the NEDD8-activating enzyme, does not result in a global reorganization of the CRL network. Examination of CRL complex stoichiometry reveals that, independent of cullin neddylation, a large fraction of cullins are assembled with adaptor modules while only a small fraction are associated with CAND1. These studies suggest an alternative model of CRL dynamicity where the abundance of adaptor modules, rather than cycles of neddylation and CAND1 binding, drives CRL network organization.

Introduction

Understanding the mechanisms through which protein networks are dynamically reorganized is not only important for a complete description of cell systems but also has important implications for the identification of pharmacological agents that affect particular pathways (Przytycka et al., 2010). Dynamic changes in networks often are provoked by post-translational modification of proteins in the network, yet even for widely studied pathways, we have little quantitative information concerning the occupancy of individual modification events and how these modifications are linked with dynamic complex reorganization. Small-molecule inhibitors of protein complex assembly or modification often alter the dynamic reorganization of signaling networks, trapping a given signaling complex in a perpetual ON or OFF state. For example, the microtubule inhibitor taxol binds to β-tubulin within assembled microtubules, thereby blocking cycles of microtubule disassembly and assembly. A barrier to understanding the dynamic nature of signaling networks is the lack of quantitative approaches for determining the occupancy of protein complexes and how this changes in response to perturbation. In this report, we globally

Address correspondence to: wade_harper@hms.harvard.edu.

Conflict of Interest Statement

J.W.H. is a consultant for Millennium Pharmaceuticals. J.R. is an employee of Cell Singaling Technolgies.

characterize the cullin-RING ubiquitin ligase (CRL) network and describe the development and use of a quantitative proteomic platform to elucidate CRL dynamics.

CRLs are modular ubiquitin ligases that control much of the regulated protein turnover in eukaryotic cells (Petroski and Deshaies, 2005). CRLs contain 3 major elements; a cullin scaffold, a RING finger protein (RBX1 or RBX2) that recruits a ubiquitin-charged E2 enzyme, and a substrate adaptor that places substrates in proximity to the E2 enzyme to facilitate ubiquitin transfer. The founding member of the CRLs, the SCF (Skp1/Cul1/F-box protein) ubiquitin ligase, recognizes substrates via an adaptor module composed of Skp1 and one of ~68 F-box proteins in humans (Jin et al., 2004). Six additional cullin (2, 3, 4A, 4B, 5, and 7)-RING complexes interact with distinct sets of adaptor modules, forming ~200 unique CRL complexes in total (Petroski and Deshaies, 2005). Central to formation of an active CRL complex is the modification of a single conserved lysine residue in the cullin subunit with the ubiquitin-like protein NEDD8 (Petroski and Deshaies, 2005; Wolf et al., 2003), which promotes the structural reorganization of the C-terminal RING binding domain of the cullin thereby promoting the processivity of ubiquitin transfer (Duda et al., 2008; Saha and Deshaies, 2008) Neddylation, or rubylation in yeast, occurs through an E1-E2-E3 cascade involving NEDD8-activating enzyme (NAE), NEDD8 E2s, cullin-associated RBX1, and the E3-like factor DCUN1D1/Dcn1p (Rabut and Peter, 2008).

CRLs are thought to represent highly dynamic assemblies that are regulated by several mechanisms (Bosu and Kipreos, 2008; Cope and Deshaies, 2003; Wolf et al., 2003). First, with dozens of substrate adaptor modules for individual cullins, the repertoire of adaptors may need to be molded for the particular needs of the cell. This could be accomplished via multiple mechanisms, including new adaptor synthesis, adaptor competition, and adaptor turnover through an autocatalytic mechanism referred to as “adaptor instability”, allowing assembly of new CRLs with distinct specificities. The rules that govern the repertoire of CRLs in particular cellular settings are largely unknown but it has been proposed that adaptor instability ensues after turnover of substrates for a specific CRL is complete (Chew and Hagen, 2007; Petroski and Deshaies, 2005; Wee et al., 2005; Wolf et al., 2003; Yang et al., 2002). Second, cullin neddylation is subject to reversal by an 8-subunit deneddylase referred to as the COP9 signalosome complex (CSN), thereby converting active CRLs to inactive forms (Cope and Deshaies, 2003; Wolf et al., 2003). COPS5, a JAMM (JAB1, MPN, MOV34) domain metalloisopeptidase, contains the catalytic site for deneddylation within the CSN (Cope et al., 2002). Third, there is evidence of a sequestration pathway that serves to inhibit the CRL pathway. This pathway involves the heat-repeat protein CAND1, which binds unneddylated adaptor-free cullin-RING complexes, thereby rendering them in an inactive form (Goldenberg et al., 2004; Liu et al., 2002; Zheng et al., 2002).

While the CSN clearly functions as a negative regulator of CRLs *in vitro* through removal of NEDD8, genetic data indicate a positive role for the CSN in CRL function *in vivo* (Bosu et al., 2010; Bosu and Kipreos, 2008; Cope and Deshaies, 2003; Hotton and Callis, 2008; Wolf et al., 2003). This apparent paradox is unresolved but has been rationalized through the idea that CRLs must undergo cycles of neddylation and deneddylation in order to be fully functional in cells. The prevailing notion is that dynamic cycling is important for interchanging adaptor modules (Figure S1F) (Bosu and Kipreos, 2008; Cope and Deshaies, 2003; Wolf et al., 2003). This model is based upon the observation that persistent CRL neddylation due to genetic CSN inactivation can promote instability of a subset of adaptors, thereby leading to inhibition of relevant signaling pathways (Cope and Deshaies, 2003). The ability of CAND1 to associate with unneddylated, adaptor-free cullins has led to a model wherein the CAND1-cullin-RING complex serves as an intermediate in the cullin neddylation cycle, with release of cullin-RING from CAND1 being necessary for assembly with an alternative adaptor module (Bosu and Kipreos, 2008). In plants and *C. elegans*

mutants in CAND1 display defects consistent with a positive role in the function of a subset of CRLs (Bosu et al., 2010; Hotton and Callis, 2008). Nevertheless, loss of CAND1 orthologs in plants, human cells, or yeast has little effect on the abundance of neddylated cullins, suggesting that the neddylation cycle may function independently of CAND1 (Chew and Hagen, 2007; Liu et al., 2002; Zhang et al., 2008; Zheng et al., 2002). Moreover, deletion of CAND1 orthologs in yeast has no effect on cell viability (Schmidt et al., 2009; Siergiejuk et al., 2009). A resolution of the cullin neddylation cycle paradox is hampered by several factors. First, the steady-state occupancy of adaptors, NEDD8, CSN, CAND1, and DCN1 on individual cullins is unknown, even in the most widely studied systems. This limitation is amplified by the virtually universal use of semi-quantitative immunoblot approaches to examine interactions, and the cellular levels of CRL components remain unknown in any system. Second, while it is generally thought that the majority of cullins *in vivo* are maintained in the unneddylated state, the actual occupancy of NEDD8 on cullins is unknown. Third, the current models suggest that acute inhibition of cullin neddylation would ultimately result in the global sequestration of cullin-RING complexes into an inactive complex with CAND1, but this model has not been rigorously tested without prolonged genetic perturbations.

In order to evaluate existing CRL dynamicity models, we have performed a systematic analysis of the human CRL regulatory network in the presence and absence of the specific NAE inhibitor MLN4924 (Soucy et al., 2009). This inhibitor makes a covalent adduct with NEDD8, leading to rapid loss of cullin neddylation in cells, followed by accumulation of CRL substrates (Brownell et al., 2010). This was accomplished by merging semi-quantitative spectral counting methods to rapidly evaluate the organization of the CRL network and determine general trends in network reorganization upon acute deneddylation with quantitative multiplex AQUA (Absolute Quantification) technology to determine the occupancy of individual components and complexes within the CRL network. We found that the distribution of CRL regulatory proteins was not uniform across the various cullin complexes, implying that individual cullin assemblies may employ distinct modes of regulation. Contrary to existing models, we found that acute inhibition of cullin neddylation does not result in a global reorganization of the CRL proteome, loss of adaptor association, or large-scale sequestration of cullins by CAND1. A large fraction of CUL1 and CUL4B are assembled with substrate adaptor modules with only a small fraction associated with CAND1, regardless of cullin neddylation status. Unexpectedly, we found that a more accurate snapshot of cellular CRL assemblies and the extent of cullin neddylation required inhibition of CSN activity upon cell lysis, implying that previous studies may have substantially underestimated the abundance of neddylated cullins. These studies suggest an alternative model of CRL control where the abundance of adaptor modules, rather than cycles of neddylation and CAND1 binding, drive the dynamic organization of the CRL network, and reveal the multiplex AQUA approach as a powerful tool to determine how the architecture of signaling networks are reorganized by perturbations.

Results

A platform for systematic proteomic analysis of the CRL regulatory network

In order to systematically explore the architecture of the CRL regulatory network, we created cells lines using retroviral induction that expressed FLAG-HA-(TAP) tagged human CUL1, CUL2, CUL4A, CUL4B, CUL5, DCUN1D1, COPS6, COPS5, NEDD8, and CAND1 in 293T cells at or below their endogenous levels (Figure S1A). TAP-CUL3 lines could not be established and was expressed using a transient lentiviral approach. Liquid chromatography-mass spectrometry (LC-MS/MS) data derived from anti-HA immune complexes was processed through *CompPASS* to identify high confidence candidate interacting proteins (Sowa et al., 2009), thereby providing a snapshot of the steady-state

CRL network. As expected, each cullin associated with specific classes of substrate adaptor proteins in addition to regulatory proteins (Figure 1A, Table S1). We found 26 F-box proteins as well as SKP1 and the SKP2 associated cyclin A-CDK-CKS complex associated with CUL1 (Figure 1B), 12 BC-Box containing and 14 SOCS-box containing proteins in addition to elongins B and C with CUL2 and CUL5, respectively (Figure 1C,F), 53 BTB containing proteins with CUL3 (Figure 1D), and 24 DCAFs along with DDB1 associated with CUL4A or CUL4B (Figure 1E). While this represents the largest number of substrate adaptors identified in a single experiment, the absence of a subset of known or predicted adaptors suggest that the CRL network identified here represents the most abundant or avidly associated adaptors in 293T cells. The hypothesis that proline at position 2 in the F-box motif is required for CUL1 association (Schmidt et al., 2009) was not confirmed, as FBXL18 and FBXO30 lacking this residue were found in association with CUL1. CAND1 associated with CUL1, CUL3, CUL4B, and CUL5, as expected (Liu et al., 2002; Zheng et al., 2002) (Figure S1B). However, the total spectral counts (TSCs) for CAND1 varied widely depending on the individual cullin (Figure 1A), indicating that CAND1 is not uniformly distributed across cullins. Only five of the seven cullins were found within NEDD8 immune complexes while 6 of the 7 cullins were present in COPS6 complexes (Figure S1C,D, Table S1). However, the distribution of cullins differed, suggesting further heterogeneity in the CRL regulatory network. For example, TSCs for CUL5 and its associated adaptor proteins were lower than other cullins within NEDD8 and COPS6 immune complexes. CAND1 was absent from not only NEDD8-associated complexes, as expected, but also from CSN complexes suggesting that CAND1 and CSN associate with distinct populations of cullin complexes (Olma et al., 2009). Six cullins were associated with DCUN1D1 (Figure S1E), with the CUL3 and CUL5 CRL complexes being the most highly represented within the DCUN1D1 complex.

CSN activity within lysates alters the architecture of the CRL network

The majority of previous studies report that only a small fraction of cullins are modified by NEDD8 (typically <10%). However, the finding that a substantial fraction of cullins are associated with the CSN deneddylase raised the possibility that CSN activity upon cell lysis reduces the apparent extent of neddylation observed. To test this possibility, we lysed TAP-CUL1 expressing cells in the presence and absence of the zinc chelator and COPS5 inhibitor 1,10-orthophenathroline (OPT) (Cope et al., 2002). TAP-CUL1 was completely unneddylated in the absence of OPT under the lysis conditions used while ~50% of CUL1 was neddylated with OPT in the lysis buffer (Figure 2A), suggesting that inhibition of CSN upon cell lysis can substantially increase the extent of CUL1 neddylation similar to what was observed when antibodies against COPS2 (CSN2) were included during lysis (Yang et al., 2002). Examination of the extent of endogenous cullin neddylation revealed that addition of OPT, but not the non-chelating 1,7-orthophenanthroline, resulted in dramatically increased levels of observable CUL1 and CUL3 neddylation and smaller increases in the amount of CUL2 and CUL4A neddylation (Figure 2B). Addition of the NAE inhibitor MLN4924 in combination with OPT to the lysis buffer did not alter the levels of cullin neddylation, indicating that the observed increase in cullin neddylation upon lysis in the presence of OPT was not due to *in vitro* NAE activity (Figure 2B). As expected, addition of MLN4924 to cells 4 hours prior to lysis resulted in complete deneddylation of all cullins (Figure 2B).

We therefore examined the impact of OPT on the global CRL network by measuring TSCs, which provide a semi-quantitative measure of protein abundance in parallel immune complexes (Figure 2C, Table S2). Only in the presence of OPT were we able to detect TSCs for all 7 cullins as well as an increase in the amount of bait normalized TSCs for individual cullins within NEDD8 immune complexes (Figure 2C,D). This effect was particularly

striking with CUL3, where capture of neddylated CUL3 is almost completely dependent on CSN inhibition (Figure 2B, D). CSN association with cullins was largely unaffected by OPT addition, except for CUL1, where CSN inhibition reproducibly increased the interaction between CSN and CUL1 (Figure 2E,F). A reduction in CAND1 TSCs associated within CUL1, CUL3, CUL4A, and DCUN1D1 was also observed, although statistical significance was reached only with CUL4A and DCUN1D1 (Figure 2G). We conclude that CSN inhibition *in vitro* via OPT addition increases the extent of CRL neddylation and more closely represents the *in vivo* status of the CRL network. As such, OPT was included in all experiments described hereafter unless otherwise noted.

MLN4924 treatment results in rapid deneddylation of CRLs

Having defined conditions that allow us to approximate the *in vivo* architecture of the CRL network using proteomics, we next examined the effects of acute inhibition of neddylation on CRL network organization. In agreement with previous reports, treatment of 293T cells with the NAE inhibitor MLN4924 (1 μM) for 4 hours resulted in complete conversion of endogenous neddylated cullins to their unneddylated forms (Figure 3A) (Soucy et al., 2009). Similarly, treatment of the TAP-tagged CRL and regulatory protein expressing cells resulted in near complete deneddylation of exogenous cullins (Figure 3B), as well as endogenous CUL5, CUL4A, and CUL1 associated with CRL regulatory proteins (Figure 3C). CUL2 and CUL5 expression can only be detected after HA immunoprecipitation (data not shown). To further validate the use of MLN4924 to examine CRL dynamics, we treated TAP-NEDD8 expressing cells with MLN4924 for 4 hours and examined the associated complexes by LC-MS/MS (Figure 3D). As expected, MLN4924 treatment resulted in a severe reduction in the association of CRL complexes with NEDD8 (Figure 3E). Bait normalized TSCs for the cullins, CSN subunits, and associated cullin adaptor proteins within NEDD8 immune complexes were largely lost upon treatment with MLN4924 (Figures 3E-G). In contrast, NEDD8 maintained its association with components of the NAE heterodimer (UBA3 and NAE1) upon MLN4924 treatment (Figure 3H) indicating that the reduction of CRLs associated with NEDD8 was due to loss of isopeptide linked NEDD8.

Acute NAE1 inhibition does not globally alter the CRL network

The prevailing models of CRL dynamics, based primarily on prolonged genetic perturbations, predicts that inhibition of cullin neddylation would result in CRL complex disassembly, release of adaptor protein modules, and sequestration of the cullin-RING complex by CAND1. In order to test the dynamic nature of CRL complexes on a short time scale, we first evaluated the effect of 4 hour MLN4924 treatment on the TAP-CRL pathway cell library (Figure 4A, Table S3). In contrast to expectations, the array of adaptor proteins associated with individual cullins based on TSCs was largely unchanged, and in the case of CUL2, several adaptor proteins displayed a statistically significant increase in association (Figure 4E). Consistent with these results, MS analysis of TAP-tagged adaptor proteins revealed stable associated with their target cullins irrespective of the neddylation status (Figure S3A, B).

In contrast with adaptor proteins, analysis of cullin regulatory components revealed distinct patterns of changes that were generally cullin specific. Inhibition of neddylation resulted in a significant (25–60%) decrease in CSN-CUL1 and CSN-CUL3 association whether examined using CSN or cullin immune complexes (Figure 4B-C), a result that was confirmed by immunoblotting (Figure 4D). Given the loss of association of CSN with cullin seen upon deneddylation, one might anticipate an increase in CAND1 association. Indeed, the extent of TAP-CAND1 association with CUL1, CUL4, and CUL5 was increased 2–8 fold as assessed by TSCs (Figure 4B). Increased CAND1 association was also seen with TAP-CUL1, CUL4A, CUL4B, CUL5, and DCUN1D1 upon inhibition of neddylation, a

result that at face value is consistent with the CAND1 sequestration model (Figure 4C). Together, this analysis revealed that while CAND1 association with cullins does increase upon deneddylation, this does not occur at the expense of global CRL complexes as the amount of adaptor containing CRL complexes was largely unchanged by NAE inhibition (Figure 4E). Of note, interrogation of the effect of NAE inhibition on the same complexes but without inhibition of CSN activity with OPT resulted in either reduction or ablation of the changes observed in regulatory protein binding to CRLs in the presence of OPT, underscoring the importance of OPT addition to allow changes in the CRL network upon deneddylation to be revealed (Figure S2, Table S4).

In order to examine the effects of acute cullin deneddylation on endogenous complexes, we immunoprecipitated endogenous CUL1 and subjected the complex to LC-MS/MS (Figure S3C). While TSCs for CUL1 were ~10-fold lower than that found with TAP-CUL1 due to antibody efficiency, we found CSN, SKP1, and 10 F-box proteins in association with endogenous CUL1. Nine of 10 F-box proteins, as well as SKP1 and CSN components, remained associated in comparable levels 4 hours after NAE inhibition, pointing to the absence of a global reorganization of the endogenous CUL1 complex.

Multiplex AQUA for quantitative proteomics of the CRL network

While we observed increased cullin-CAND1 association upon deneddylation using spectral counting, it is not possible to use this technique to determine CAND1-cullin stoichiometry. In order to provide a quantitative picture of CRL architecture upon deneddylation and to determine the occupancy of individual subunits within the network, we developed a multiplex AQUA platform for the CRL network. We synthesized a library of 38 reference tryptic peptides corresponding to peptides previously observed by LC-MS/MS for each of the cullins, SKP1, DDB1, CSN subunits, CAND1, DCUN1D1, NEDD8, and the F-box proteins BTRC (β-TRCP1) and FBXW11 (β-TRCP2) (Figure 5A, Table S6). Each reference peptide contained a single $N^{15}C^{13}$ labeled amino acid, allowing heavy and endogenous (light) peptides to be distinguished and quantified by MS (Kirkpatrick et al., 2005). For 10 of 23 target proteins, we identified 2 or 3 useful peptides, while for 12 targets, single reference peptides were available. Trypsin digested CRL complexes were supplemented with 100 fmoles of the peptide library prior to LC-MS/MS and the relative intensities of extracted ion chromatograms from endogenous and reference peptides from duplicate MS runs were used to calculate the abundance of the endogenous protein within each immune complex. For those proteins with multiple reference peptides the average ratio among the reference peptides is reported (Table S5). Reference and endogenous NEDD8 peptide was readily observed within TAP-CUL1 immune complexes in untreated cells but MLN4924 treatment resulted in complete loss of the endogenous NEDD8 peptide while the intensities of the NEDD8 reference peptide and peptides for CUL1 itself were unchanged (Figure 5B). Using this technique we determined the mole fraction of CUL1 associated with each CRL regulatory component.

Consistent with immunoblots, ~45% of CUL1 is neddylated under steady state conditions, and this fraction is lost, as expected, with MLN4924 treatment (Figure 5C). Interestingly, multiplex AQUA analysis of CUL1 purified without OPT in the lysis buffer revealed only 5% of CUL1 to be neddylated, consistent with immunoblotting results here and in other studies (Figure 2B, S4A,B). It is possible that OPT-mediated CSN inhibition may not be absolute in cell lysates and thus our measurement of the extent of neddylation may underestimate that in intact cells. Further, we observed a greater than 3-fold increase in the amount of NEDD8 associated with CSN immune complexes as well as the amount of cullins associated with TAP-NEDD8 immune complexes upon inclusion of OPT in lysis conditions (Figure S4A,B). Surprisingly, only a small fraction (6%) of CUL1 was associated with CAND1 in the absence of MLN4924 and this increased to 13% upon deneddylation (Figure

5C). The CUL1/CSN fraction represented 26% of the total CUL1 in untreated cells and this decreased to 10% upon NAE1 inhibition. For simplicity, unless otherwise noted all CSN measurements represent the average mole fraction calculated from multiplex AQUA analysis of all CSN subunits (15 peptides). Interestingly, the majority (73%) of CUL1 was associated with SKP1 and this fraction increased slightly after MLN4924 treatment (Figure 5C). This suggests that the majority of CUL1 is potentially occupied with F-box proteins under steady state conditions, and acute deneddylation of the cullin does not decrease this fraction contrary to the prevailing model. Analogous measurements of TAP-CUL1 expressed in HeLa cells (Figure 5D) revealed a smaller fraction of neddylated CUL1 (8%), and somewhat reduced levels of CSN and SKP1 (6 and 50%, respectively) when compared to 293T cells. As observed with 293T cells, deneddylation led to a ~2-fold reduction in CSN binding to CUL1. In contrast, 13% of CUL1 was associated with CAND1 and this did not appreciably change upon deneddylation (Figure 5D). In both 293T and HeLa cells, we found that CUL1, CUL3, CUL4A, and CUL4B are the most abundant cullins associated with TAP-NEDD8 (Figure S4B,D). Further, the absolute amount of SKP1 and CUL1 present within NEDD8 immune complexes from 293T cells is equivalent, indicating that the entirety of the neddylated cullin fraction also contains SKP1 (Figure S4B).

Neddylation is dispensable for CUL1 complex assembly but is required for CAND1 association

To investigate the requirement of neddylation on complex assembly by proteomics, we created cells with inducible expression of non-neddylatable $CUL1^{K720R}$ or CUL1 dominant negative ($CUL1^{DN}$). $CUL1^{DN}$ binds SKP1-F-box protein complexes but does not interact with either CAND1 or CSN, and therefore serves as a control for adaptor assembly. Western blotting confirmed that $CUL1^{K720R}$ was not neddylated (Figure 6B). We found that $CUL1^{K720R}$ assembled with CSN, SKP1, and a majority of F-box proteins to the same extent as wild-type CUL1 (Figure 6A). As seen previously (Liu et al., 2002), $CUL1^{K720R}$ displayed a 10-fold reduction in CAND1 binding compared to wild-type CUL1 (Figure 6C). $CUL1^{DN}$ associated with F-box proteins, but as expected, did not bind CSN or CAND1 (Figure 6C,D). Quantitative MS analysis confirmed that $CUL1^{K720R}$ was deficient in CAND1 binding, leading to an increase in the mole fraction of total CUL1 associated with SKP1 approaching 100% (Figure 6E). Compared to MLN4924 treated CUL1, $CUL1^{K720R}$ bound 2-fold more CSN despite both complexes being completely deneddylated and suggesting that CSN can interact with CRLs independent of prior neddylation (Figure 6E). As seen by spectral counting, $CUL1^{K720R}$ associated with the F-box proteins BTRC (β-TRCP1) and FBXW11 (β-TRCP2), albeit reduced by 2-fold compared to wild-type CUL1 as measured by AQUA (Figure 6E). To confirm that F-box proteins similarly associated with wild-type CUL1 and $CUL1^{K720R}$ we transiently expressed five FLAG-tagged-F-box proteins with either wild-type MYC-CUL1 or MYC-$CUL1^{K720R}$. Subsequent FLAG immunoblotting of the MYC-IP revealed no difference in F-box binding between wild-type and neddylation-defective CUL1 (Figure S5). Further, MLN4924 treatment of cells expressing wild-type MYC-CUL1 also showed no decrease in ability to associate with co-expressed F-box proteins confirming that acute deneddylation does not affect F-box protein association with CUL1 (Figure S5A).

Absence of global reorganization of the CRL network upon prolonged deneddylation

The neddylation cycle paradox emerges from the finding that the CSN functions to positively regulate CRL function *in vivo*. As such, we considered the possibility that the absence of global reorganization of the CRL network in the experiments presented thus far reflect the relatively short time period (4h) allowed for reorganization after NAE inhibition. However, the mole fraction of TAP-CUL1 associated with SKP1, CSN, and CAND1 was essentially static from 2 to 16 hours of MLN4924 treatment (Figure 6F,G). Immunoblotting

of cell extracts revealed complete loss of neddylation after 2h of MLN4924 treatment with a concomitant increase in the abundance of the well-characterized CUL3/KEAP1 substrate NRF2 (Figure 6F). Over 70% of CUL1 was associated with SKP1 in untreated cells, and this level was maintained 16 hours after NAE inhibition. Thus, even upon prolonged deneddylation, CUL1-based CRL complexes are not globally converted to a CUL1-CAND1 complex, as would be predicted by the current model.

Quantitative assessment of CUL1 complexes upon depletion of COPS5, CAND1 or SKP1

Previous reports suggested that reduction of COPS5 or CAND1 levels resulted in hyperactivation of CRLs leading to the inappropriate degradation of unstable adaptor proteins thereby paradoxically inactivating CRL function (Hotton and Callis, 2008). It therefore remained possible that reduction of CSN or CAND1 may have large affects on CRL network architecture not seen after acute NAE1 inhibition. Using siRNA oligos targeting either the catalytic COPS5 subunit or CAND1, we achieved a 90% reduction of COPS5 levels with one of the two siRNA oligos and a similar reduction of CAND1 levels with both siRNA duplexes (Figure S5B). Surprisingly, the amount of neddylated CUL1 was largely unaffected despite greater than 90% reduction in either COPS5 or CAND1 levels. This unexpected result may reflect the lack of OPT in previous experiments, which underestimated the amount of neddylated cullins in control treated samples. Quantitative assessment of CUL1 complexes after knockdown revealed that loss of COPS5 did not result in a significant loss of association with the larger CSN complex (Figure S5D) despite a reduction in the amount of the COPS5 subunit associated with CUL1, which is in agreement with previous studies (Figure S5B,D) (Sharon et al., 2009). The fraction of CAND1 bound to CUL1 remained at similar levels in control knockdown cells compared to knockdown of COPS5. As expected, knockdown of CAND1 resulted in a 3-fold reduction in the amount of CAND1 bound to CUL1 and a concomitant increase in the amount of SKP1 bound to CUL1 from 62% in untreated cells to 75% after CAND1 depletion (Figure S5C). Knockdown of CAND1 had no affect on the amount of total CSN bound to CUL1 (Figure S5C). These results suggest that genetic reduction of CSN activity does not alter the overall CRL stoichiometry and that the fraction of the adaptor assembled ligase versus the inhibited CAND1 bound complex can be altered by lowering CAND1 levels.

We also examined the effect of depletion of SKP1 on CSN and CAND1 association with HA-CUL1 (Figure S5C,E). With three of four siRNAs targeting SKP1, there was a ~40% reduction in the mole fraction of CUL1 associated with SKP1 not seen with control siRNA or the ineffective SKP1 siRNA oligo 1. This was accompanied by an increase in the fraction of CUL1 bound to CAND1 (from ~6% to ~50%) (Figure S5E). This data is consistent with mutually exclusive binding of SKP1 and CAND1 to CUL1, and reveals that SKP1 binding predominates *in vivo*.

Application of multiplex AQUA for assessment of CRL occupancy

The modular nature of CRL complexes and the presence of variable regulatory proteins allows for the construction of a wide variety of heterogeneous assemblages. For example, when considering only NEDD8, CAND1, CSN, and SKP1 as possible CUL1 interacting proteins, it is possible to envision 9 distinct CRL assemblies (Figure 7A). While this does not consider the heterogeneity of the different F-box proteins, we assume that assemblies containing SKP1 represents complexes that are potentially assembled with F-box proteins. The quantitative nature of AQUA allowed us to determine the contribution of each of these species to the total occupancy of CUL1. Under steady-state conditions in 293T cells, ~19% of CUL1 is unoccupied whereas greater than 70% contains SKP1, of which the majority is neddylated (Figure 7B). Note that we are unable to identify RBX1 peptides in association with CUL1 and for the purposes of this discussion, we expect that what we refer to as

unoccupied CUL1 is actually associated with RBX1. In previous studies (Olma et al., 2009; Wolf et al., 2003) and here, almost half of the CSN bound fraction of CUL1 does not contain NEDD8 suggesting that either CSN remains associated with CUL1 after deneddylation or neddylation is not required for CSN binding. As CSN associates with neddylation-deficient CUL1 (Figure 6C), we favor the latter possibility. MLN4924 treatment resulted in a complete loss of all neddylated species and a decrease in the amount of unoccupied CUL1 to 3.8%, reflecting increased SKP1 and CAND1 binding. Analogous measurement of CUL1 occupancy from TAP-CUL1 expressed in HeLa cells revealed an increase in the amount of unoccupied CUL1 resulting from the observed reduction of CUL1 neddylation as compared to 293T cells (Figure S6C). This suggests that CRL occupancy and possibly the mechanisms that govern CRL assembly may vary between cell types.

Occupancy determinations for CUL4B expressed in 293T cells revealed quantitative differences in CUL4B occupancy as compared to CUL1 complexes. CUL4B was neddylated to a similar extent as CUL1 but contained less bound DDB1 and CAND1, ~40% and 1%, respectively, but more CSN, ~40%, compared to CUL1 (Figure 7C). As such, we observed an adaptor-free CSN bound CUL4B complex at steady-state conditions, an assembly not seen in CUL1 complexes (Figure 7C). Conversion of CUL4B to a completely unneddylated state by MLN4924 addition did not substantially alter the fraction of CUL4B bound to CSN, DDB1, or, surprisingly, CAND1. However, MLN4924 treatment dramatically increased the amount of completely unoccupied CUL4B at the expense of the neddylated, but otherwise uncomplexed, CUL4B fraction. Examination of CUL4A expressed in HeLa cells revealed CUL4A occupancy to be nearly identical to CUL4B expressed from 293T cells (Figure S4C,S6D).

We also determined the fraction of CSN occupied by cullins measured from TAP-COPS6 or TAP-COPS5 complexes. In untreated cells, cullins occupy 60% and 40% of the total COPS6 or COPS5, respectively (Figure 7D). The total occupancy decreases with MLN4924 treatment but is more apparent in COPS5. The decrease in COPS5 occupancy relative to COPS6 likely reflects the presence of a large monomeric pool of COPS5 (Tomoda et al., 2002). Interestingly, CUL4B represents the largest fraction of cullins bound to CSN with 38% occupancy of COPS6 compared to CUL1 with 9% occupancy (Figure 7D). This underscores our finding that CRL association with CSN varies depending upon the individual CRL complex examined.

Finally, we also measured the fraction of CAND1 that is in complex with cullins. Consistent with spectral counting (Figure 4), CUL1, CUL4B, and CUL5 represent 95% of the cullins in complex with CAND1 (Figure 7E). Interestingly, less than half of the total CAND1 was in complex with cullins and this percentage increased to only 57% after treatment with MLN4924 (Figure 7E). Thus, unneddylated cullins are not converted to cullin-CAND1 complexes despite the presence of available CAND1, suggesting that additional regulatory events may be required to facilitate assembly of CAND1 onto unneddylated adaptor-loaded CRL complexes. CAND1 occupancy increased to 85% when OPT was omitted from the lysis buffer (Figure S6A), indicating that excess CAND1 is available to bind to *in vitro* CSN mediated deneddylated cullins. Taken together our data necessitates a redefinition of the dynamic model of CRL regulation where upon translation, CUL1 is assembled with SKP1 which in turn is neddylated and CRL activity is modulated by successive cycles of CSN mediated deneddylation and NAE1 dependent neddylation without intervening sequestration by CAND1 (Figure 7F).

Discussion

CRLs and the neddylation cycle

Over a decade of research on CRL function and regulation has elucidated the molecular identity of each of the individual CRL complexes as well as the myriad of cellular pathways CRLs impinge upon (Petroski and Deshaies, 2005). However, a quantitative snapshot of the CRL network landscape has yet to be accomplished. By utilizing a quantitative multiplex AQUA approach, we provide the first description of CRL occupancy and the effect of acute deneddylation on CRL network architecture. To our knowledge, our study is the first to apply this strategy to elucidate the occupancy of multi-protein networks of this complexity and how these networks are altered by pathway perturbations. As such, the precise determination of CRL occupancy determined in this study will likely be further refined as quantitative mass spectrometry techniques improve. It should be noted that, while validated in many systems, utilization of tryptic peptides as surrogates for proteins may not precisely reflect protein abundances (Kirkpatrick et al., 2005) (see Supplemental Methods).

Cullin neddylation, and by extension CRL activity, is antagonized by both CSN-mediated deneddylation and CAND1-mediated cullin sequestration *in vitro*, while both CSN and CAND1 are needed for optimal *in vivo* CRL activity in eukaryotes (Bosu and Kipreos, 2008; Cope and Deshaies, 2003; Wolf et al., 2003). Current models invoke a neddylation-CAND1 cycle wherein deneddylated and adaptor-free cullin is sequestered by CAND1 and this complex is then used to build new cullin complexes with a different adaptor molecule (Figure S1F). A central prediction of the model is that persistent cullin deneddylation would result in loss of adaptor proteins from cullins and concomitant global sequestration of cullins by CAND1. However, our analysis of CRL network architecture with and without cullin neddylation fail to validate this model in 293T and HeLa cells, and suggests that substrate adaptor levels play a central role in dictating the architecture of the CRL network (Figure 7F).

An alternative model for CRL dynamics revealed by quantitative proteomics

For simplicity, we describe an alternate model in the context of the SCF (Figure 7F) but we envision similar mechanisms will apply for other CRLs. Newly synthesized CUL1-RING assembles with adaptor complexes, which then promote CUL1 neddylation (Bornstein et al., 2006; Chew and Hagen, 2007). Once assembled, the SCF complex can associate with the CSN complex, and this can occur, in principal, with unneddylated cullin as exemplified by the $CUL1^{K720R}$ mutant. However, given the decrease in CSN association with CUL1 seen after acute deneddylation, we favor a model wherein CSN preferentially or initially associates with neddylated forms of CRLs. Association of CSN complexes with both neddylated and unneddylated cullins suggests that binding of the CSN to the CRL is not rate-limiting for deneddylation and implies additional regulatory steps dictating NEDD8 removal from cullins. A large fraction of CUL1 (~70% in 293T cells) is in complex with SKP1 (and presumably F-box proteins) independent of the neddylation status, suggesting that the assembly and activation pathway is dominant for the SCF. In this model, the formation of SCF complexes is driven primarily by adaptor binding, and CAND1 does not play a direct role in the assembly or re-assembly process.

We found that only a small fraction of cullins are associated with CAND1 in 293T cells and association increases by less than 2-fold in response to acute deneddylation (Figure S6B), indicating a minor role for CAND1 in the bulk steady-state dynamic remodeling of CRL complexes. However, it is clear that CAND1 function is needed for CRL activity in multicellular eukaryotes (Bosu and Kipreos, 2008; Hotton and Callis, 2008), leading to the obvious question: What is CAND1 doing? An answer to this question will likely require the

elucidation of the forms of cullins that serve as targets for CAND1 binding. The simplest possibility is that newly synthesized CUL1 that escapes productive interaction with SKP1 serves as the primary target for CAND1 (Figure 7F pathway A), a scenario that is reinforced by our finding that depletion of SKP1 leads to a concomitant increase in the fraction of CUL1 bound to CAND1. In this case, the cellular concentration of SKP1 dictates the proportion of adaptor assembled CUL1. Alternatively, CUL1 that has previously been assembled with adaptor complexes and neddylated may be the source of CUL1 found in complexes with CAND1. This possibility is suggested by the finding that non-neddylatable $CUL1^{K720R}$ does not efficiently bind CAND1 *in vivo*, despite the fact that CAND1 interacts with a large surface area on CUL1 (Goldenberg et al., 2004) (Figure 7F). We envision two possible scenarios for CAND1 sequestration of previously assembled and neddylated CUL1. In one scenario, CUL1 that was previously associated with a small subset of specific F-box proteins (Adaptor Z in Figure 7F, pathway B) might be selected for CAND1 sequestration. In principle, this subset could represent adaptor proteins that are subject to adaptor instability or some other form of regulation that marks that CUL1 scaffold for CAND1 sequestration. In the second scenario, CAND1 may target CUL1 independently of the identity of the previously associated F-box protein, but given the CAND1 occupancy on CUL1, only a small fraction of the total CUL1 pool would be shunted into this pathway (Figure 7F, pathway C). The finding that a small fraction of CUL1 is associated with CAND1 even in the absence of neddylation would favor pathway B and would explain why loss of CAND1 function may result in phenotypes reflecting the activity of a particular F-box protein without affecting global CRL architecture. In support of this model, loss of CAND1 function in *C. elegans* resulted in reduction of specific CRL functions while leaving others unaffected (Bosu et al., 2010). Further studies are required to identify relevant pools of cullins that are assembled into CAND1 complexes and signals that control CAND1 sequestration. Moreover, further studies are required to determine whether the “free” pool of CAND1 identified by AQUA and its association with cullins is regulated. Our studies examine the CRL network in asynchronous cells. It is also possible that CAND1 restricts CRL activity upon a specific cell stimulus, state, or lineage where CRL activity may need to be inhibited beyond CSN-mediated deneddylation. Indeed, we have found that the extent CUL1 neddylation in HeLa cells is ~4-fold lower than that seen in 293T cells (Figure 5C,D) yet only ~14% of CUL1 is associated with CAND1 independent of neddylation status. Interestingly, our analysis of CRL components in 293T cell extracts using multiplex AQUA (Figure S6E) revealed that the concentration of cullins is in excess of NEDD8, suggesting that the extent of CRL neddylation may be limited by the available pool of free NEDD8. This finding is in agreement with the observation that nearly all NEDD8 exits in a conjugated form (Brownell et al., 2010). Unlike SKP1, the DDB1 concentration in extracts is below that of the combined CUL4A and CUL4B concentrations. This may explain why we observe a larger portion of CUL4B that does not have adaptors bound compared to CUL1 (Figure 7B,C). However another possibility is that, while validated in many systems, utilization of tryptic peptides as surrogates for proteins may not precisely reflect protein abundances (Kirkpatrick et al., 2005) (see Supplemental Methods).

While this work suggests a major role for substrate adaptor modules in dictating the architecture of the CRL network, several major issues are left unresolved. Are adaptor modules in rapid equilibrium with cullins or once an adaptor is associated with a cullin, is it essentially irreversibly bound during the lifetime of the CRL complex? Moreover, given that inhibition of NAE leads to rapid deneddylation, it would appear that the neddylation and deneddylation systems are poised to dynamically regulate the extent of CRL neddylation on very short time scales. What then is the biological role of such dynamic control under physiological conditions, given the apparent absence of a role of neddylation in assembly of substrate adaptors on cullins? Finally, what role does cell lineage play in dictating the abundance of factors that control on and off rates for neddylation? The answers to these

questions will likely require the development of *in vitro* systems that fully recapitulate the dynamics of CRL assembly seen *in vivo*. Finally, this work suggests that multiplex AQUA provides a powerful approach for elucidating how cellular perturbations affect the organization of signaling networks.

Experimental Procedures

Plasmids, cell lines, and protein purification

Details of the retroviral plasmids (Sowa et al., 2009), cell culture procedures, and antibodies used can found in the Supplemental Methods. Four 15cm dishes expressing a given TAP-CRL protein (with or without incubation with MLN4924 (provided by Millennium Pharmaceuticals) were harvested and lysed with 3mL lysis buffer (50mM Tris pH 7.5, 150mM NaCl, 0.5% NP-40, and Complete protease inhibitor tablet (Roche)). Where indicated 2mM 1,10-orthophenathroline or 1,7-orthophenathroline (Sigma) was added to the lysis buffer. Cleared lysates were filtered through 0.45 μm, spin filters (Millipore Ultrafree-CL) and immunoprecipitated with 30 μl α-HA resin (Sigma). Endogenous α-CUL1 complexes were washed and digested with trypsin on beads.

Mass Spectrometry and quantitative analysis

Immunoprecipitated complexes were washed 3X with lysis buffer, exchanged into PBS, and eluted with 150μL of 250μg/ml HA peptide in PBS. Eluted complexes were precipitated with 10% Trichloroacetic acid (TCA, Sigma) and pellets were washed 3X with cold acetone. TCA precipitated proteins were resuspended in 50mM ammonium bicarbonate pH8.0 with 10% acetonitrile and sequencing grade trypsin (promega) at a concentration of 12.5ng/μl. Trypsin reactions were quenched by addition of 5% formic acid and peptides were desalted using the C18 stagetip method. Tandem MS/MS data was searched using Sequest and a concatenated target-decoy IPI human database with a 2Da mass window for data generated using LTQ linear ion trap mass spectrometer (ThermoFinnigan) or LTQ-Velos and a 50ppm mass window for data generated using an LTQ-Orbitrap (ThermoFinnigan) instrument. All data was filtered to a 1% false discovery rate (peptide level) prior to analysis using *CompPASS* (Sowa et al., 2009).

For multiplex AQUA analysis, samples were resuspended with 100 fmoles of a library of $N^{15}C^{13}$–labeled reference peptides (see Table S6; (Kirkpatrick et al., 2005)) in 5% acetonitrile, 5% formic acid prior to analysis on an LTQ-Orbitrap. HPLC purified AQUA reference peptides (Table S6) were quantified using colorimetric detection of primary amines by 2,4,6-Trinitrobenzene sulfonic acid (TNBSA, Pierce) (See Supplemental Methods). The ratios of extracted ion chromatograms for reference and endogenous peptide precursor ions (mass window = 20 ppm) were obtained using *PINPOINT* software (Thermo) (see Table S5). Endogenous protein concentrations for the indicated CRL components were determined from LTQ-Orbitrap analysis of 1μg of 293T whole cell extract. Due to the low intensity of some endogenous peptide ions in whole cell extract digests, ion chromatogram ratios were determined by manual inspection of MS chromatograms.

RNAi

TAP-CUL1 cells were transfected with 20nM siRNA duplexes (Dharmacon/Thermo) using RNAiMAX (Invitrogen) according to manufacturer guidelines. Cells were harvested 72 hours after transfection and processed for western blotting or mass spectrometry analysis.

Supplementary Material

Refer to Web version on PubMed Central for supplementary material.

Acknowledgments

We thank Woong Kim, Ryan Kunz, and Fiona McAllister from the Gygi laboratory (Harvard Medical School) for assistance with the AQUA analysis, Harper lab members John Lydeard for reagents, Mat Sowa for bioinformatics assistance, and Brenda O'Connell for a critical reading of the manuscript. This work was supported by grants to J.W.H. from Millennium Pharmaceuticals, the National Institutes of Health, and the Stewart Trust. E.J.B. is a Damon Runyon Fellow supported by the Damon Runyon Cancer Research Foundation (DRG 1974-08)

References

Bornstein G, Ganoth D, Hershko A. Regulation of neddylation and deneddylation of cullin1 in SCFSkp2 ubiquitin ligase by F-box protein and substrate. Proc Natl Acad Sci U S A. 2006; 103:11515–11520. [PubMed: 16861300]

Bosu DR, Feng H, Min K, Kim Y, Wallenfang MR, Kipreos ET. C. elegans CAND-1 regulates cullin neddylation, cell proliferation and morphogenesis in specific tissues. Dev Biol. 2010; 346:113–126. [PubMed: 20659444]

Bosu DR, Kipreos ET. Cullin-RING ubiquitin ligases: global regulation and activation cycles. Cell Div. 2008; 3:7. [PubMed: 18282298]

Brownell JE, Sintchak MD, Gavin JM, Liao H, Bruzzese FJ, Bump NJ, Soucy TA, Milhollen MA, Yang X, Burkhardt AL, et al. Substrate-assisted inhibition of ubiquitin-like protein-activating enzymes: the NEDD8 E1 inhibitor MLN4924 forms a NEDD8-AMP mimetic in situ. Mol Cell. 2010; 37:102–111. [PubMed: 20129059]

Chew EH, Hagen T. Substrate-mediated regulation of cullin neddylation. J Biol Chem. 2007; 282:17032–17040. [PubMed: 17439941]

Cope GA, Deshaies RJ. COP9 signalosome: a multifunctional regulator of SCF and other cullin-based ubiquitin ligases. Cell. 2003; 114:663–671. [PubMed: 14505567]

Cope GA, Suh GS, Aravind L, Schwarz SE, Zipursky SL, Koonin EV, Deshaies RJ. Role of predicted metalloprotease motif of Jab1/Csn5 in cleavage of Nedd8 from Cul1. Science. 2002; 298:608–611. [PubMed: 12183637]

Duda DM, Borg LA, Scott DC, Hunt HW, Hammel M, Schulman BA. Structural insights into NEDD8 activation of cullin-RING ligases: conformational control of conjugation. Cell. 2008; 134:995–1006. [PubMed: 18805092]

Goldenberg SJ, Cascio TC, Shumway SD, Garbutt KC, Liu J, Xiong Y, Zheng N. Structure of the Cand1-Cul1-Roc1 complex reveals regulatory mechanisms for the assembly of the multisubunit cullin-dependent ubiquitin ligases. Cell. 2004; 119:517–528. [PubMed: 15537541]

Hotton SK, Callis J. Regulation of cullin RING ligases. Annu Rev Plant Biol. 2008; 59:467–489. [PubMed: 18444905]

Jin J, Cardozo T, Lovering RC, Elledge SJ, Pagano M, Harper JW. Systematic analysis and nomenclature of mammalian F-box proteins. Genes Dev. 2004; 18:2573–2580. [PubMed: 15520277]

Kirkpatrick DS, Gerber SA, Gygi SP. The absolute quantification strategy: a general procedure for the quantification of proteins and post-translational modifications. Methods. 2005; 35:265–273. [PubMed: 15722223]

Liu J, Furukawa M, Matsumoto T, Xiong Y. NEDD8 modification of CUL1 dissociates p120(CAND1), an inhibitor of CUL1-SKP1 binding and SCF ligases. Mol Cell. 2002; 10:1511–1518. [PubMed: 12504025]

Olma MH, Roy M, Le Bihan T, Sumara I, Maerki S, Larsen B, Quadroni M, Peter M, Tyers M, Pintard L. An interaction network of the mammalian COP9 signalosome identifies Dda1 as a core subunit of multiple Cul4-based E3 ligases. J Cell Sci. 2009; 122:1035–1044. [PubMed: 19295130]

Petroski MD, Deshaies RJ. Function and regulation of cullin-RING ubiquitin ligases. Nat Rev Mol Cell Biol. 2005; 6:9–20. [PubMed: 15688063]

Przytycka TM, Singh M, Slonim DK. Toward the dynamic interactome: it's about time. Brief Bioinform. 2010; 11:15–29. [PubMed: 20061351]

Rabut G, Peter M. Function and regulation of protein neddylation. 'Protein modifications: beyond the usual suspects' review series. EMBO Rep. 2008; 9:969–976. [PubMed: 18802447]

Saha A, Deshaies RJ. Multimodal activation of the ubiquitin ligase SCF by Nedd8 conjugation. Mol Cell. 2008; 32:21–31. [PubMed: 18851830]

Schmidt MW, McQuary PR, Wee S, Hofmann K, Wolf DA. F-box-directed CRL complex assembly and regulation by the CSN and CAND1. Mol Cell. 2009; 35:586–597. [PubMed: 19748355]

Sharon M, Mao H, Boeri Erba E, Stephens E, Zheng N, Robinson CV. Symmetrical modularity of the COP9 signalosome complex suggests its multifunctionality. Structure. 2009; 17:31–40. [PubMed: 19141280]

Siergiejuk E, Scott DC, Schulman BA, Hofmann K, Kurz T, Peter M. Cullin neddylation and substrate-adaptors counteract SCF inhibition by the CAND1-like protein Lag2 in Saccharomyces cerevisiae. Embo J. 2009; 28:3845–3856. [PubMed: 19942853]

Soucy TA, Smith PG, Milhollen MA, Berger AJ, Gavin JM, Adhikari S, Brownell JE, Burke KE, Cardin DP, Critchley S, et al. An inhibitor of NEDD8-activating enzyme as a new approach to treat cancer. Nature. 2009; 458:732–736. [PubMed: 19360080]

Sowa ME, Bennett EJ, Gygi SP, Harper JW. Defining the human deubiquitinating enzyme interaction landscape. Cell. 2009; 138:389–403. [PubMed: 19615732]

Tomoda K, Kubota Y, Arata Y, Mori S, Maeda M, Tanaka T, Yoshida M, Yoneda-Kato N, Kato JY. The cytoplasmic shuttling and subsequent degradation of p27Kip1 mediated by Jab1/CSN5 and the COP9 signalosome complex. J Biol Chem. 2002; 277:2302–2310. [PubMed: 11704659]

Wee S, Geyer RK, Toda T, Wolf DA. CSN facilitates Cullin-RING ubiquitin ligase function by counteracting autocatalytic adapter instability. Nat Cell Biol. 2005; 7:387–391. [PubMed: 15793566]

Wolf DA, Zhou C, Wee S. The COP9 signalosome: an assembly and maintenance platform for cullin ubiquitin ligases? Nat Cell Biol. 2003; 5:1029–1033. [PubMed: 14647295]

Yang X, Menon S, Lykke-Andersen K, Tsuge T, Di X, Wang X, Rodriguez-Suarez RJ, Zhang H, Wei N. The COP9 signalosome inhibits p27(kip1) degradation and impedes G1-S phase progression via deneddylation of SCF Cul1. Curr Biol. 2002; 12:667–672. [PubMed: 11967155]

Zhang W, Ito H, Quint M, Huang H, Noel LD, Gray WM. Genetic analysis of CAND1-CUL1 interactions in Arabidopsis supports a role for CAND1-mediated cycling of the SCFTIR1 complex. Proc Natl Acad Sci U S A. 2008; 105:8470–8475. [PubMed: 18550827]

Zheng J, Yang X, Harrell JM, Ryzhikov S, Shim EH, Lykke-Andersen K, Wei N, Sun H, Kobayashi R, Zhang H. CAND1 binds to unneddylated CUL1 and regulates the formation of SCF ubiquitin E3 ligase complex. Mol Cell. 2002; 10:1519–1526. [PubMed: 12504026]

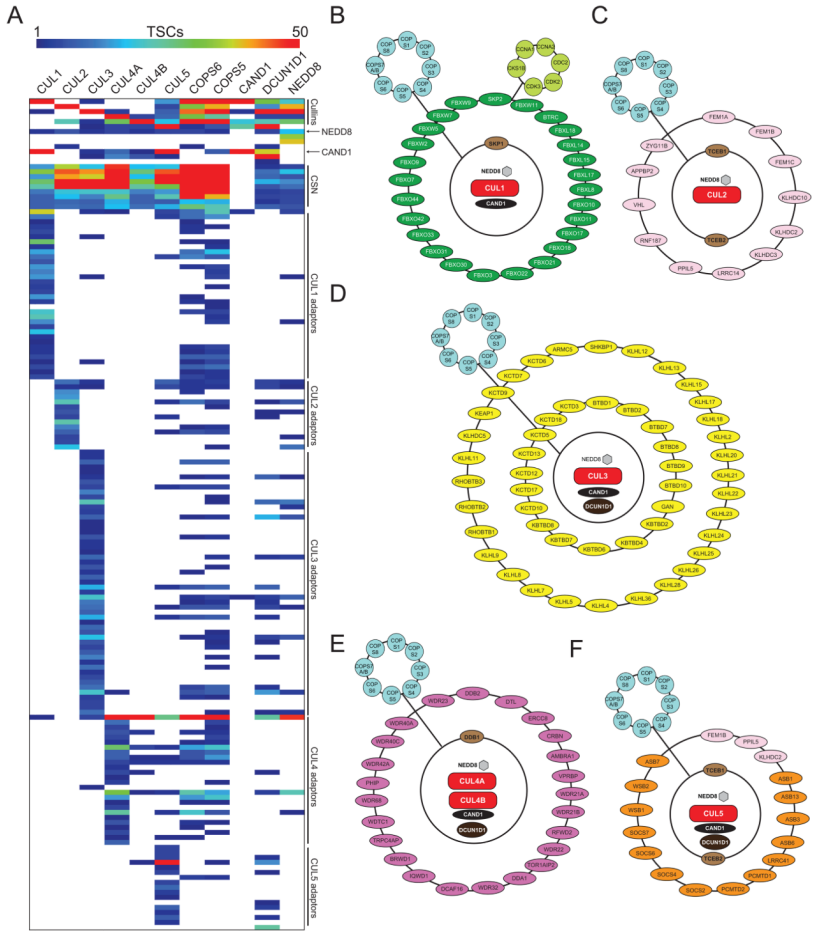

Figure 1. Systematic proteomic analysis of the CRL network at steady-state

(A) TSCs for CRL components associated with each bait are indicated by the heat map. Associated proteins are depicted within the heat map if the TSCs for the given protein were in excess of 3. For a complete list of interacting proteins see Table S1.

(B-F) Schematic representation of proteins associated with CUL1(B), CUL2(C), CUL3(D), CUL4A or CUL4B(E) and CUL5(F). See also Figure S1.

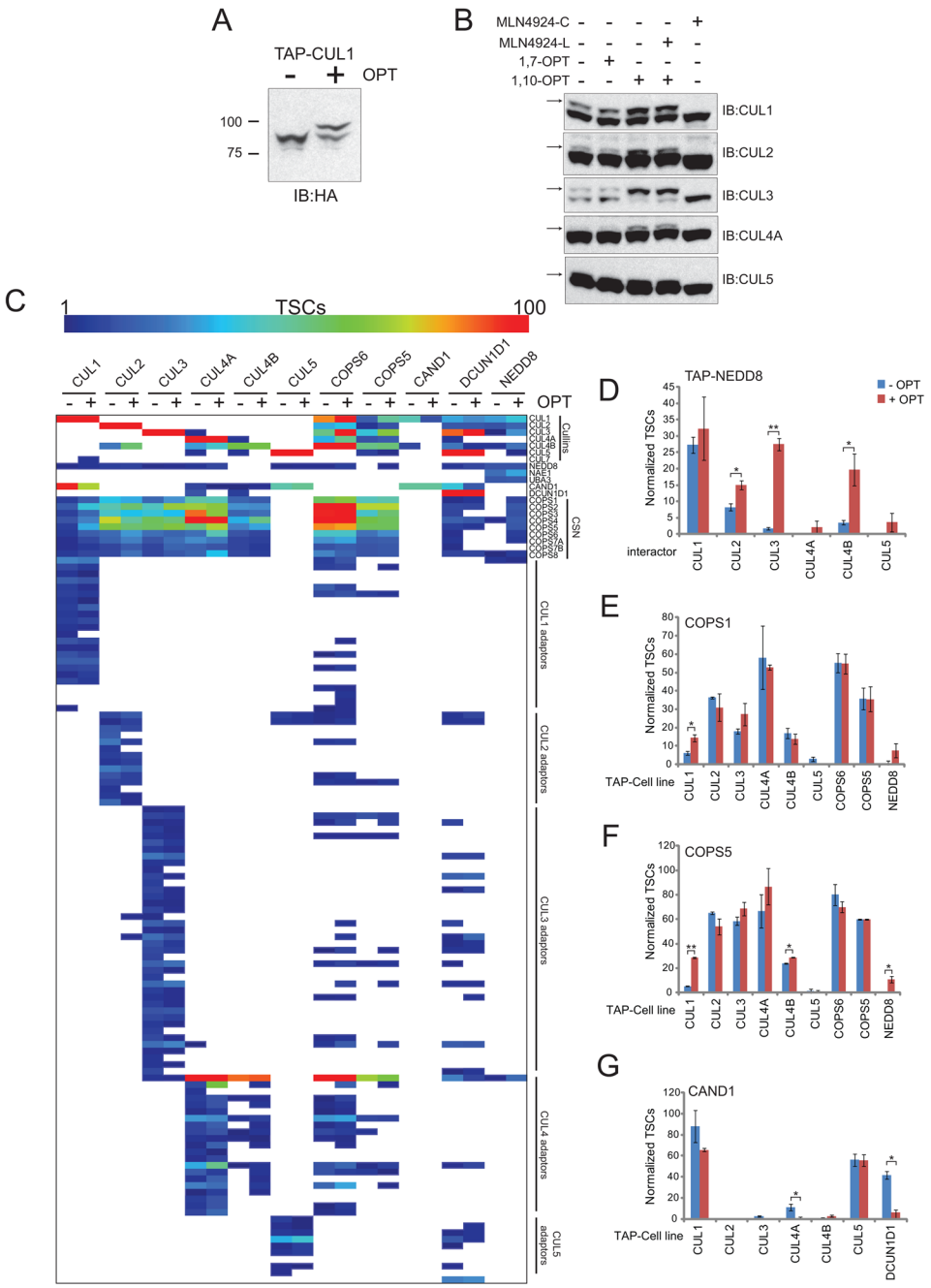

Figure 2. CSN activity within lysates alters the architecture of the CRL network

(A) TAP-CUL1 cells were lysed in the presence or absence of 2mM 1,10 o-phenanthroline (OPT) and analyzed by SDS-PAGE and immunoblotted with α-HA antibodies.

(B) 293T cells were either untreated or treated with 1μM MLN4924 for 4 hours (MLN4924-C). Untreated cells were then lysed without OPT, with 1–10 OPT, 1–7 OPT, or 1–10 OPT with MLN4924 added to the lysis buffer (MLN4924-L). The extent of cullin neddylation was determined by immunoblotting. Arrows indicate the neddylated species.

(C) LC-MS/MS analysis of the indicated immune complexes in the presence or absence of OPT. TSCs were normalized by bait TSCs. Associated proteins are depicted within the heat

map if the TSCs for the given protein were in excess of 3 within any of the immune complexes.

(D) Comparison of cullin TSCs within TAP-NEDD8 immune complexes with (red bars) or without OPT (blue bars) in the lysis buffer.

(E-G) Bait normalized TSCs for COPS1(E), COPS5(F), or CAND1(G) associated with the indicated TAP-immune complexes with (red bars) and without OPT (blue bars) in the lysis buffer. Error bars: STDEV of duplicate measurements (*,** = pvalue < 0.05, 0.01, respectively, by Student's t-test). See also Figure S2 and Table S2.

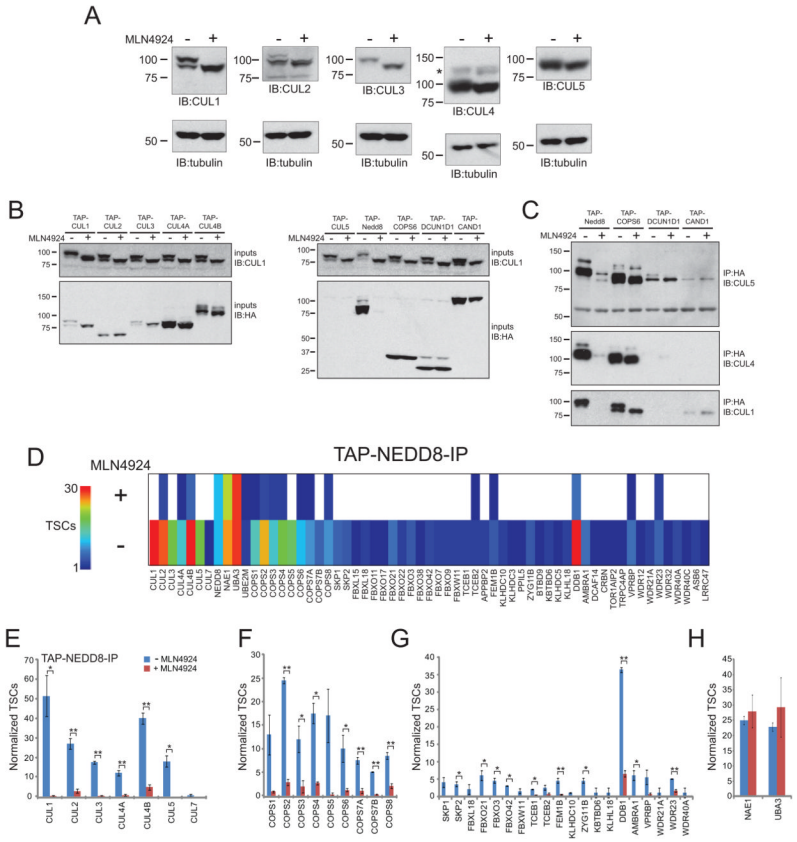

Figure 3. Rapid deneddylation of CRLs in response to NAE inhibition by MLN4924

(A) 293T cells with or without 1μM MLN4924 (4h) treatment were lysed in the presence of OPT and the extent of neddylation of endogenous cullins was determined by immunoblotting. *indicates non-specific background band.

(B) 293T cells expressing the indicated TAP-tagged proteins with or without 4h MLN4924 treatment were lysed in the presence of OPT and immunoblotted with the indicated antibodies. Bait complexes were immunoprecipitated with α-HA and immunoblotted with the indicated antibodies.

(C) Complexes were immunoprecipitated with α-HA coupled resin and blotted with antibodies against CUL1, CUL5, and CUL4A.

(D) TAP-NEDD8 expressing cells with or without 4h MLN4924 treatment were lysed in the presence of OPT. α-HA complexes were analyzed by LC-MS/MS and bait normalized TSCs for known CRL components are displayed.

(E-H) Normalized TSCs for cullins (E), CSN subunits (F), CRL adaptor proteins (G), and the NEDD8 conjugation machinery (H) associated with TAP-NEDD8 with (red bars) or without (blue bars) MLN4924 treatment. Error bars: STDEV of duplicate measurements (*,** = pvalue < 0.05, 0.01, respectively, by Student's t-test).

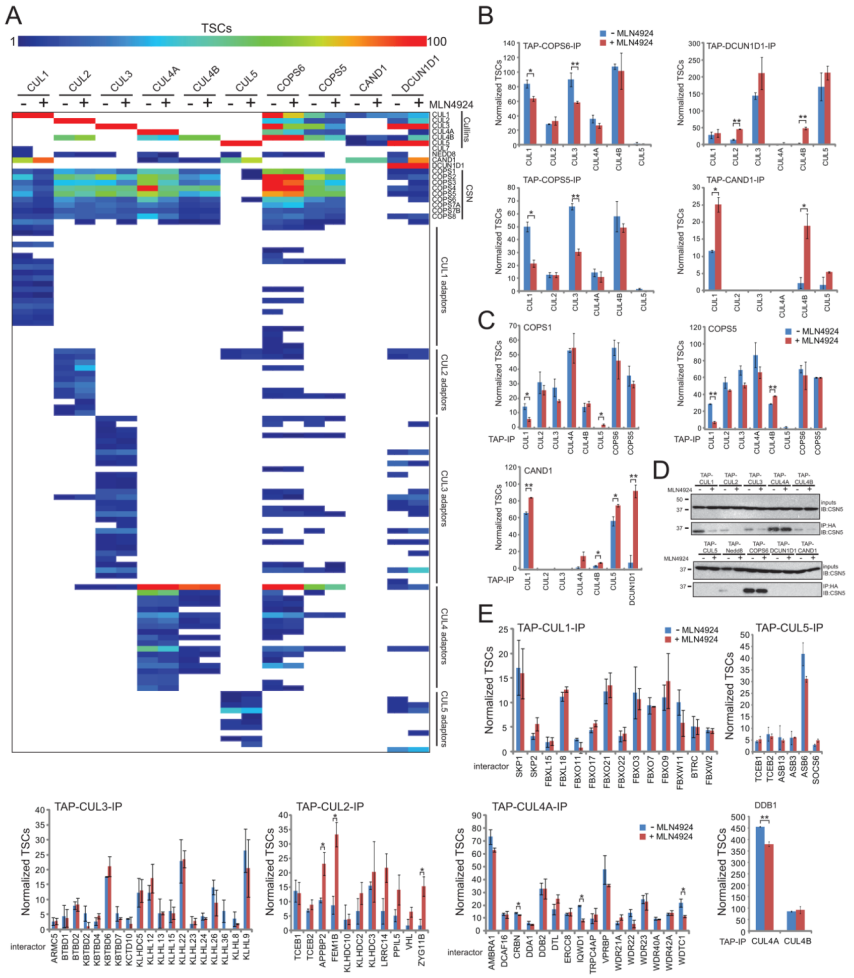

Figure 4. Acute NAE1 inhibition does not globally alter the CRL network

(A) Extracts from 293T cells expressing the indicated proteins (with or without 4h MLN4924 treatment) were immunoprecipitated with α-HA and associated proteins were identified by LC-MS/MS. Bait-normalized TSCs for associated CRL components are shown.

(B) The relative abundance of cullins associated with CSN6, DCUN1D1, COPS5, or CAND1 immune complexes with (red bars) or without (blue bars) MLN4924 treatment.

(C) Normalized TSCs for COPS1, COPS5, or CAND1 associated with the indicated immune complexes with (red bars) and without MLN4924 (blue bars) treatment.

(D) Extracts from 293T cells expressing the indicated proteins (with or without 4h MLN4924 treatment) were probed with antibodies against COPS5. Bait complexes were immunoprecipitated with α-HA and immunoblotted for COPS5.

(E) Bait normalized TSCs for a subset of adaptor proteins associated with their cognate cullin with (red bars) and without MLN4924 (blue bars) treatment. Error bars: STDEV of duplicate measurements (*,** = pvalue < 0.05, 0.01, respectively, by Student's t-test). See also Figure S3 and Table S3.

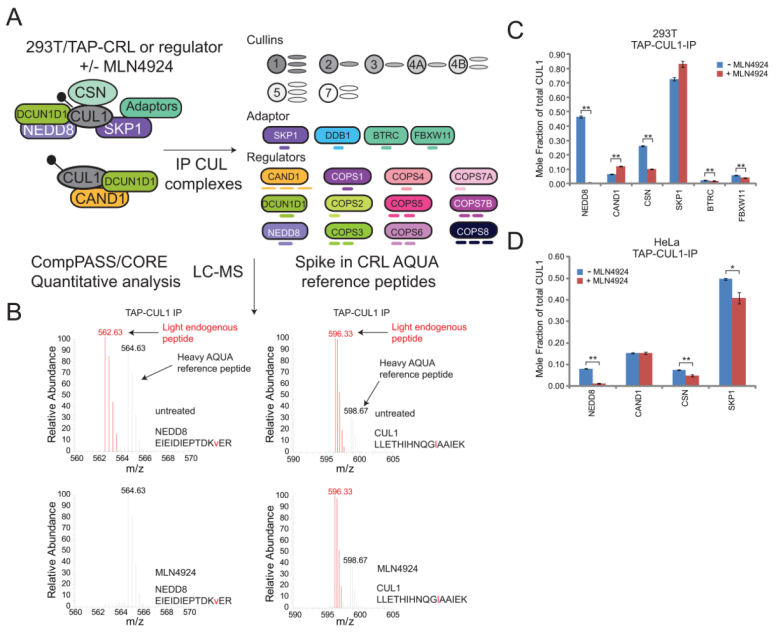

Figure 5. Multiplex AQUA for quantitative proteomics of the CRL network

(A) Schematic multiplex AQUA-based workflow. TAP-CUL1 was immunoprecipitated, eluted, and digested with trypsin. After peptide desalting, 100 fmoles of heavy-labeled AQUA reference peptide library targeting the indicated CRL components were added prior to LC-MS analysis. The colored lines under each CRL component indicate the number of AQUA peptides for that particular protein utilized in this study. See also Table S6.

(B) MS chromatogram showing a heavy reference peptide (black) and its corresponding endogenous light peptide (red) for NEDD8 (left) and CUL1 (right) before (top) and after (bottom) MLN4924 treatment present within TAP-CUL1 immune complexes. m/z values are shown together with the corresponding peptide sequence (heavy labeled amino acid in red).

(C) The concentration of the indicated components within TAP-CUL1 immune complexes from 293T cells was determined using multiplex AQUA. The mole fraction of CUL1 was then calculated by the ratio of abundances of the individual components and CUL1 with (red bars) and without MLN4924 (blue bars) treatment. CSN represents the average mole fraction calculated from AQUA measurements against each of the CSN subunits.

(D) The mole fraction of TAP-CUL1 expressed in Hela cells bound to individual CRL components with (red bars) and without MLN4924 (blue bars) treatment. Error bars: STDEV of duplicate measurements (*,** = pvalue < 0.05, 0.01, respectively, by Student's t-test). See also Figure S4.

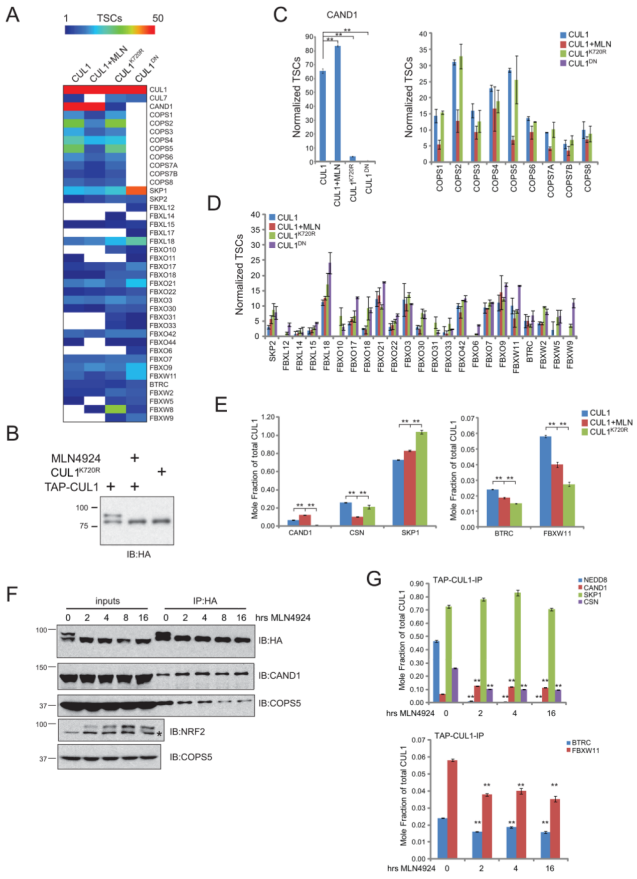

Figure 6. Quantitative proteomic analysis of neddylation deficient CUL1 complexes and time course analysis of CUL1 complexes with MLN4924 treatment

(A) Bait normalized TSCs of selected CRL components associated with wildtype TAP-CUL1 (with or without 4h MLN4924 treatment), a $CUL1^{K720R}$ mutant, and dominant negative CUL1 ($CUL1^{DN}$).

(B) HA-immunoblot of lysates from cells stably expressing wildtype TAP-CUL1 (with or without 4h MLN4924 treatment) or TAP-$CUL1^{K720R}$.

(C) Normalized TSCs for CAND1 (left) and CSN subunits (right) present in wildtype untreated and MLN4924 treated TAP-CUL1, TAP-$CUL1^{K720R}$, and TAP-$CUL1^{DN}$ immune complexes.

(D) Normalized TSCs for a subset of F-box proteins present in wildtype untreated (blue bars) and MLN4924 treated (red bars) TAP-CUL1, TAP-$CUL1^{K720R}$ (green bars), and TAP-$CUL1^{DN}$ (purple bars) immune complexes.

(E) Multiplex AQUA analysis showing the mole fraction of the indicated CUL1 associated proteins present in untreated (blue bars) and MLN4924 treated (red bars) TAP-CUL1, and TAP-$CUL1^{K720R}$ (green bars) HA-immune complexes.

(F) Extracts from 293T cells expressing TAP-CUL1 (with or without 1μM MLN4924 treatment for 2, 4, 8, or 16 h) were either immunoblotted directly or α-HA immune complexes were probed with the indicated antibodies. *indicates non-specific background band.

(G) (top) Multiplex AQUA analysis of TAP-CUL1 immune complexes from (F) showing the mole fraction of NEDD8 (blue bars), CAND1 (red bars), SKP1 (green bars), and CSN (purple bars) bound to CUL1 with increasing time of MLN4924 treatment. (bottom) Multiplex AQUA analysis of TAP-CUL1 immune complexes from (F) showing the mole

fraction of BTRC (blue bars) and FBXW11 (red bars) bound to CUL1. Error bars: STDEV of duplicate measurements (*,** = pvalue < 0.05, 0.01, respectively, by Student's t-test, comparison between untreated and MLN time points) See also Figure S5.

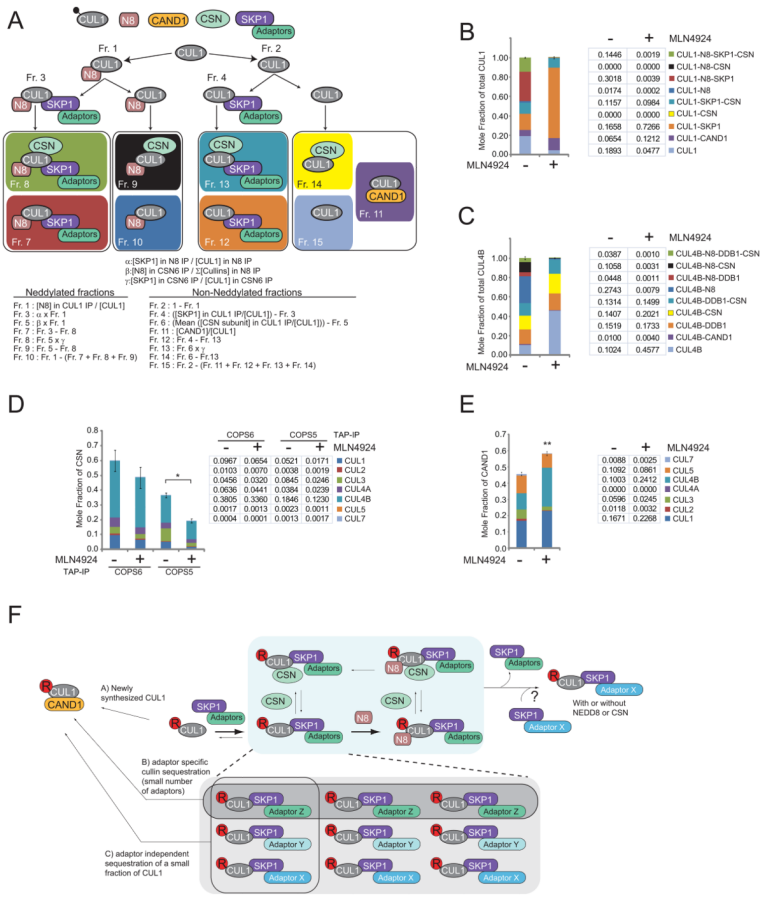

Figure 7. Application of multiplex AQUA for assessment of CRL occupancy

(A) Schematic diagram using the CUL1 CRL as an example to show how each of the 9 different assemblages are calculated using multiplex AQUA measurements. The formulas used to calculate the abundance of each fraction are depicted.

(B) The contribution of each of the assemblages depicted in (A) to the total occupancy of TAP-CUL1 immune complexes with and without MLN4924 treatment. The colors correspond to the colored assemblages in A.

(C) The occupancy of TAP-CUL4B complexes calculated as in A, except that DDB1 replaced SKP1. The ratio of DDB1 to CUL4B in NEDD8 immune complexes represents the ratio of DDB1 to the combined concentrations of CUL4A and CUL4B. The colors correspond to the colored fractions in A.

(D) Multiplex AQUA analysis of the mole fraction contribution of each of the 7 cullins associated with TAP-COPS6 (left) or TAP-COPS5 (right) with or without MLN4924 treatment.

(E) Multiplex AQUA analysis of the mole fraction contribution of each of the 7 cullins associated with TAP-CAND1 with or without MLN4924 treatment. Error bars: STDEV of duplicate measurements.

(F) Refined model of CRL dynamicity.